# Geological Insights from Malaysia Airlines Flight MH370 Search

A rich trove of marine geophysical data acquired in the search for missing flight MH370 is yielding knowledge of ocean floor processes at a level of detail rare in the deep ocean.

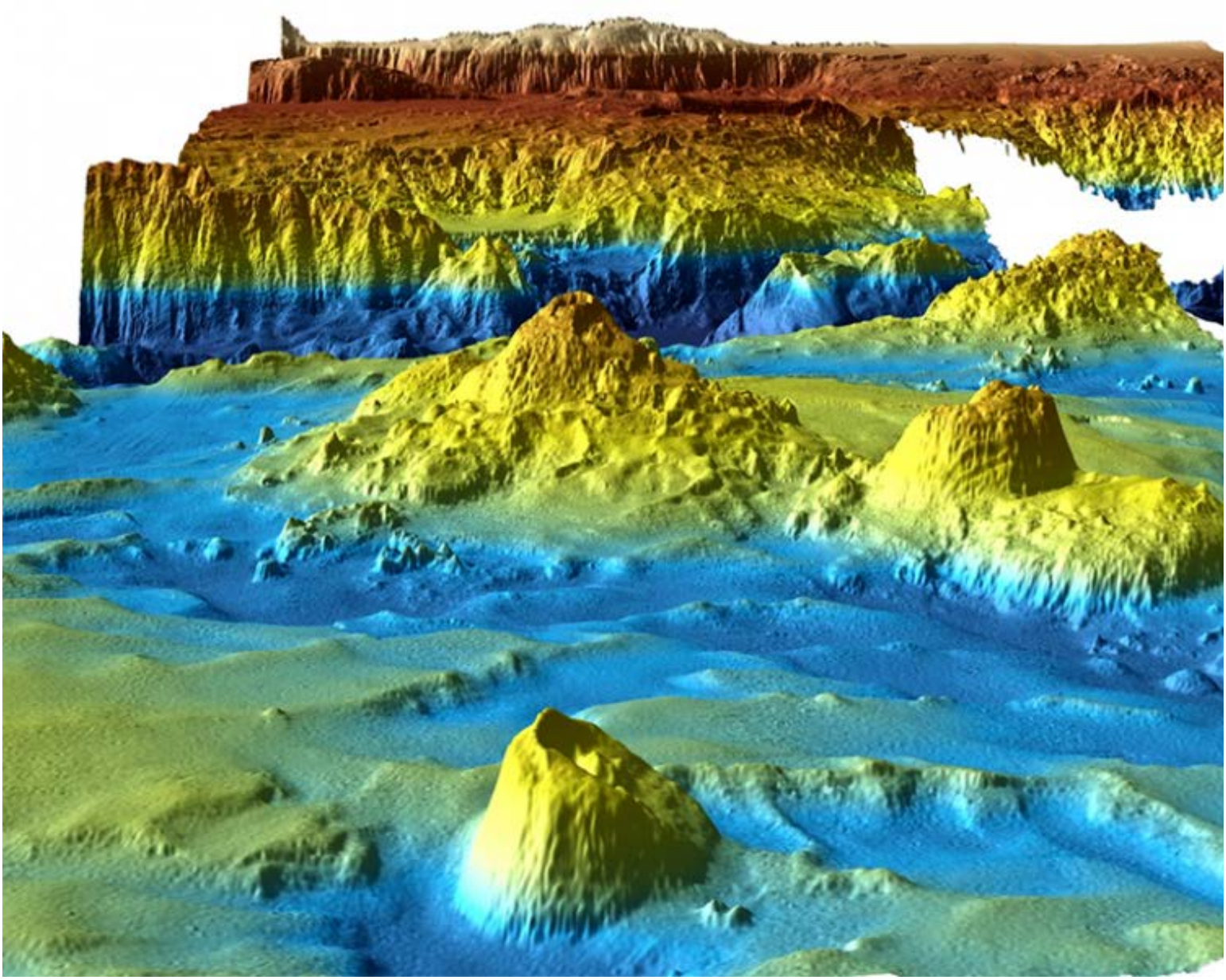

One by-product of the search for the missing Malaysian Airlines flight MH370 is a view with an unprecedented level of detail of the landscape deep in the Indian Oc 3-D image shows the Diamantina Escarpment, looking northwest (upslope). The largest seamount in this area, about 1.5 kilometers high, appears in the foreground middle and background, the escarpment and trough mark the northern margin of the rift. Vertical exaggeration is 3 times. Credit: Kim Picard and Jonah Sullivan.

By Kim Picard, Brendan Brooke, and Millard F. Coffin 6 March 2017

The tragic disappearance of Malaysia Airlines flight MH370 (http://onlinelibrary.wiley.com/doi/10.1002/2014EO210001/abstract) on 8 March 2014 led to a deep-ocean search unprecedented scale and detail. Between June 2014 and June 2016, geophysical survey teams aboard ships used echo sounding techniques to create state-of-the-art the seafloor topography and profiles of the sediments below the ocean floor in a zone spanning about 279,000 square kilometers of the southeastern Indian Ocean.

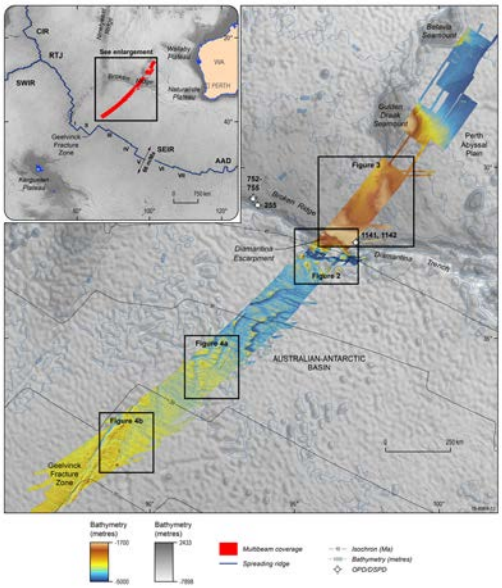


(https://eos.org/?attachment_id=69033)

Fig. 1. Satellite-derived gravity field (gray) [*Sandwell et al.,* 2014] and multibeam echo sounder (color) data were used to produce these maps of the MH370 search area in the southeast Indian Ocean. The relief models are shown in Sun-illuminated (shaded relief) mode. The inset map shows the MH370 search area that was mapped with multibeam echo sounding (shown in red). This map highlights the Southeast Indian Ridge (SEIR) and the Kerguelen Plateau, and it includes estimated spreading rates of the SEIR [*Argus et al.,* 2011], lines delineating regions of approximately equal age (isochrons [*Müller et al.,* 2008]), and interpretations of SEIR segments (I–VII [*Small et al.,* 1999]). Other abbreviations are AAD, Australian-Antarctic Discordance; CIR, Central Indian Ridge; RTJ, Rodriguez Triple Junction; SWIR, Southwest Indian Ridge; WA, Western Australia. The larger map shows details of the ocean depth mapping effort using multibeam echo sounder bathymetry data. Locations of Deep Sea Drilling Project (Leg 26) and Ocean Drilling Program (Legs 121 and 183) Sites 255, 752 to 755, 1141, and 1142 are also indicated, as are the locations of Figures 2, 3, and 4. Click image for larger version.

The curved search swath is 75 to 160 kilometers wide, and it sweeps from northeast to southwest. It centers on Broken Ridge and extends roughly 2500 kilometers f eastern flank of Batavia Seamount to the Geelvinck Fracture Zone (Figure 1). Aircraft debris found along the shores of the western Indian Ocean is consistent with d modeling that indicates the aircraft entered the sea in the search area (https://www.atsb.gov.au/mh370/).

The data set that emerged from this search effort constitutes the largest high-resolution multibeam echo sounder (http://www.ga.gov.au/about/projects/marine/mh370-bathy survey/mh370-multibeam-sonar) (a type of sonar) mapping effort for the Indian Ocean, covering an area about the size of New Zealand. Previous ocean floor maps in this had an average spatial resolution (pixel size) of more than 5 square kilometers, but the new maps resolve features smaller than 0.01 square kilometer (an area slight than a soccer field). Crucially, the new data provided the geospatial framework for the last phase of the search (http://www.ga.gov.au/about/projects/marine/mh370-bathymet in which search teams deployed deepwater, high-resolution acoustic and optical imaging instruments with the ability to identify aircraft wreckage.

## A Sharper Focus on the Ocean Floor

The global ocean covers 71% of Earth's surface, yet the ocean floor remains poorly studied compared to the land surface. In particular, knowledge of ocean floor topo sparse because light cannot penetrate the deep ocean and acoustic mapping techniques are relatively inefficient in mapping its floor. Most of the ocean floor (85%–9 been mapped indirectly using satellite-derived gravity data, which yield a spatial resolution of about 5 kilometers [*Weatherall et al.*, 2015]. By comparison, topograp of even the most remote land areas on Earth resolve features approximately 50 meters across, and topographic maps of the Moon, Mars (https://eos.org/research-spotligh mars-got-its-layered-north-polar-cap), and Venus resolve 100-meter features [*Copley*, 2014].

The high-resolution multibeam echo sounder data set that emerged from this search effort covered an area about the size of New Zealand.

Ship-mounted multibeam echo sounders that use sound waves that echo off the ocean floor provide much finer and more accurate topographic data (https://eos.org/pr updates/new-insights-from-seafloor-mapping-of-a-hawaiian-marine-monument) for the deep ocean floor with a spatial resolution (as distinct from a vertical resolution) of at least 5000-meter water depths. However, only 10%–15% of the ocean basins have been mapped using multibeam echo sounders [*Weatherall et al.*, 2015].

This technique also records acoustic backscatter from the ocean floor, which can be used to distinguish between hard rock and soft sediment. Such fundamental spa information is essential for characterizing the physical features of the ocean floor, for making inferences on geological and oceanographic processes, and for identify habitats of species that live on the ocean floor.

## A Complex Region

Beyond the continental margins, toward the open sea, the floor of the Indian Ocean is a complex mosaic of normal oceanic crust (not associated with hot spots and anomalies), submarine plateaus and ridges, seamounts (https://eos.org/project-updates/a-name-directory-for-the-ocean-floor), sea knolls, and microcontinents. Various proces including seafloor spreading (including ridge jumps (http://www.nongnu.org/magellan/magellan_ridgejump.html)), flood and hot spot magmatism, and tectonism, produce a features.

Only 10%–15% of the ocean basins have been mapped using multibeam echo sounders.

The MH370 search area includes all of the major elements of the mosaic, and it lies in water depths between 635 and 6300 meters (Figure 1). The search teams map of the area with a 30-kilohertz multibeam echo sounder system (Kongsberg EM302, M/V *Fugro Equator*), and they mapped much smaller areas with 12-kilohertz s which can reach the deeper ocean floor (Kongsberg EM122, M/V *Fugro Supporter*; Reson SeaBat 8150, Chinese PLA Navy ship *Zhu Kezhen*).

Here we highlight three examples from this shipboard multibeam echo sounder data set that are helping to illuminate the geologic development of this portion of th Ocean.

## Submarine Plateau Rifting and Breakup

Broken Ridge and the Kerguelen Plateau formed mostly as a contiguous large igneous province (http://www.largeigneousprovinces.org/) in Cretaceous time (http://www.ucmp.berkeley.edu/mesozoic/cretaceous/cretaceous.php) [*Coffin et al.*, 2000]. They subsequently experienced rifting and were eventually separated by seafloor sp along the Southeast Indian Ridge (SEIR) 43 million years ago [*Mutter and Cande*, 1983].

The southern flank of Broken Ridge, known as the Diamantina Escarpment, documents the rifting, plunging more than 5100 meters from its crest (638 meters of w into a deep trough (5800 meters of water depth). This rifted flank includes escarpments (http://www.nationalgeographic.org/encyclopedia/escarpment/)rising more than 100 the ocean floor, slopes as steep as 67°, and fault blocks about 12 by 25 kilometers in size and rising more than 1200 meters above their base (Figure 2).

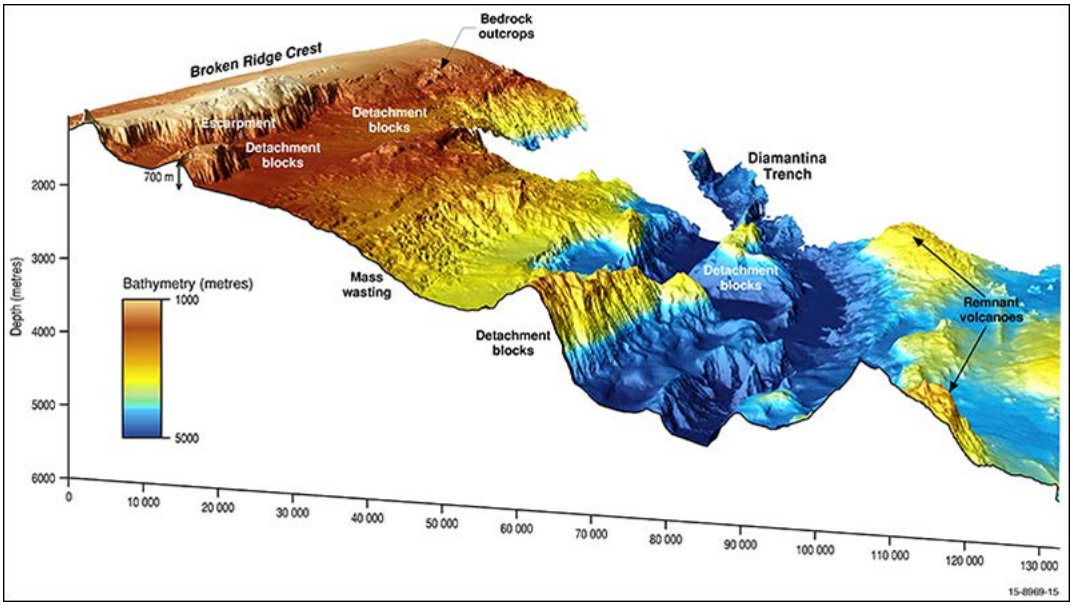


Fig. 2. Three-dimensional model looking east of the rifted southern flank of Broken Ridge (northern part of the rift valley) along the Diamantina Escarpment. Slopes commonly exceed 10°, and they increase to more than 35°

along the margins of the Diamantina Trench. Large-scale ocean floor features include escarpments (as much as 1200 meters high), detachment blocks, grabens, and areas of planar floor within the trench as wide as 10 kilometers. High backscatter intensity and angular morphology indicate that bedrock is exposed in a few places at and near the top of the ridge and on the flank down to depths of about 1350 meters. Parallel WSW–ENE lineations on some scarps, extending to water depths of about 2400 meters, most likely represent exposed steeply dipping bedding planes. Mass wasting, a downslope movement of loose rocks and sediment during and after the rifting process, has incised the escarpment, and significant sediment has accumulated in the grabens and at the bottom of the Diamantina Trench (see Figure 1 for location).

The new multibeam echo sounder data, integrated with preexisting seismic reflection and drilling data, illuminate exposed igneous basement rock, prerift sediment sections, and overlying sediment that accumulated on the ocean floor during (hemipelagic sediment) and after (pelagic sediment) rifting.

The morphology and seismic stratigraphy of the Diamantina Escarpment indicate that the mode of rifting resembled an orthogonal rift model, in which faults devel to the axis of spreading. Between the faults, a series of elongated blocks of crustal material, grabens, steps down into a deep trough and abuts the spreading ridge vo [*Karner and Driscoll*, 1993].

## Seafloor Erosion

North of its rifted southern flank, Broken Ridge generally has subtle relief, with igneous basement rocks overlain by sedimentary rock and pelagic sediment [e.g., *Co* 2000]. In places, slides and debris flows have reworked sediment downslope.

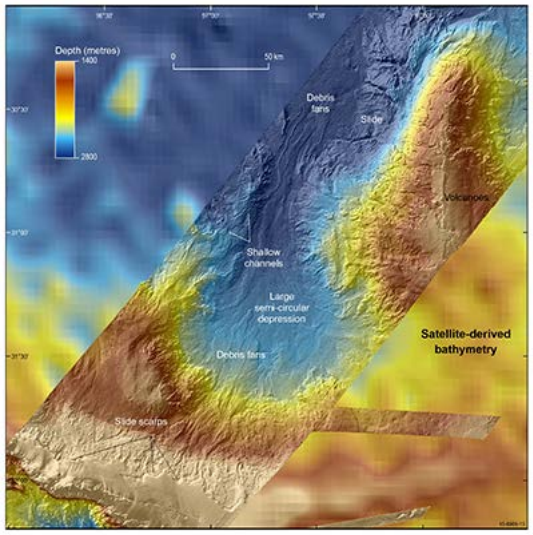


Fig. 3. The differences in resolution between multibeam and satellite-derived bathymetry data for the northern flank of Broken Ridge are apparent here. Numerous mass wasting features are evident, including slides and debris flows (delineated by their head scarps) that crosscut and run out as debris fans into the large semicircular depression (see Figure 1 for location).

A large depression, about 90 kilometers in diameter and with about 500 meters of relief, lies some 70 kilometers northeast of the crest of Broken Ridge (Figure 3). M crosscutting retrogressive slides (where the collapsing area extends progressively higher up the slope) and debris flows dissect the flanks of the depression, recordin of sediment flow, with slide scarps as much as 180 meters high and 10 kilometers wide and debris fans more than 150 kilometers long.

## Tectonic Spreading Fabric

South of Broken Ridge, normal oceanic crust of the Australian-Antarctic Basin has formed along the SEIR at intermediate spreading rates of 59–75 millimeters per [*Small et al.*, 1999; *Müller et al.*, 2008]. The shipboard multibeam echo sounder data swath traverses a region of crust north of the SEIR that is some 10 to 40 millio old, obliquely cutting across tectonic seafloor spreading fabric consisting of elongated abyssal ridges and fracture zones (Figure 1).

Oceanic crust in this region, which lies in water depths of 2200 to 5000 meters, is characterized by SEIR and paleo-SEIR segments some 200 to 500 kilometers lon 1) [*Small et al.*, 1999]. In the search area, fracture zone valleys are as much as 900 meters deep and 12 kilometers wide. The abyssal ridges have as much as 200 met relief and are more than 70 kilometers long (Figure 4).

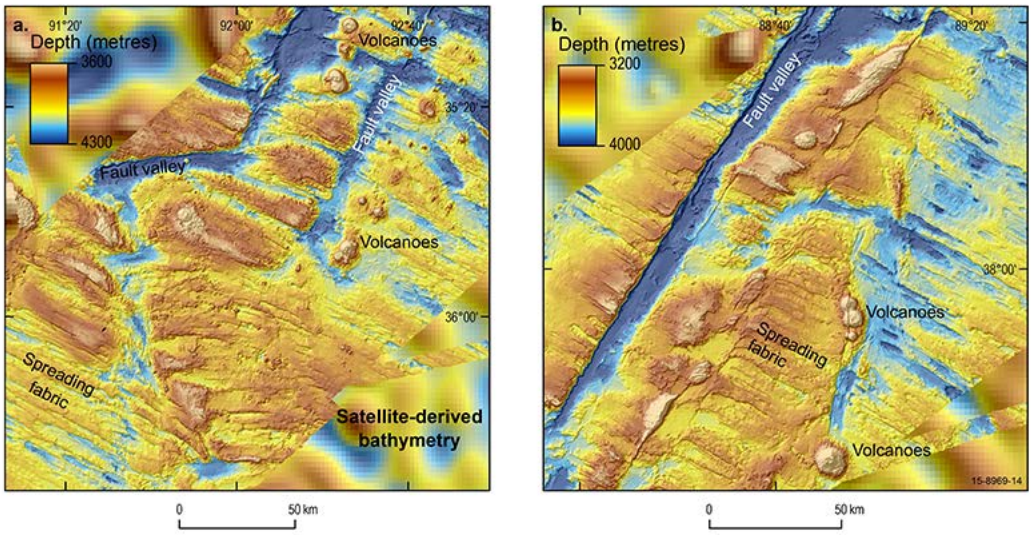


Fig. 4. Multibeam echo sounder bathymetry map of two regions of the ocean floor around the Geelvinck Fracture Zone in the Australian-Antarctic Basin south of Broken Ridge (see Figure 1 for locations). The fracture zone offsets the SEIR by about 310 kilometers (Figure 1, inset). The right-lateral transform fault motion (a person standing on one side of the fault would see the opposite side displaced to the right) that created this fracture zone was mostly horizontal. Note the fracture zone fault valleys, mid-ocean ridge spreading fabric, and isolated volcanoes.

Discontinuities along the paleo-SEIR not associated with transform faults and more than 150 sea knolls and seamounts are also common (Figure 4). Volcanoes occu isolation and in chains, forming semiconcentric structures, some as high as 1500 meters, with diameters of about 500 meters to more than 15 kilometers and slopes 10° to 30°.

## Gaining Useful Knowledge from a Tragic Event

The new data highlight the topographic complexity of the ocean floor and provided a framework for deploying deepwater instruments in the search for MH370 wrec The new multibeam echo sounder data highlight the topographic complexity of the ocean floor and provided a framework for deploying deepwater instruments in th for MH370 wreckage. The data also revealed details of the tectonic, sedimentary, and volcanic processes that formed this region of the ocean. This effort demonstrat breadth and depth of knowledge that will be gained as the remaining 85% to 90% of the global ocean is mapped at similar resolution.

## Acknowledgments

We thank the Geoscience Australia team, especially Tanya Whiteway and Maggie Tran, for project management; Maggie Tran, Justy Siwabessy, Michele Spinoccia, Sullivan, and Jonathan Weales for data processing and mapping; and Silvio Mezzomo and David Arnold for the figures. We are thankful for insightful reviews by Sc and Ron Hackney of Geoscience Austrialia and two anonymous reviewers. The search for MH370 was managed by the Australian Transport Safety Bureau and the J Agency Coordination Centre for the Malaysian government. We thank the Fugro Survey Pty. Ltd. team from Perth, Australia, and the masters and crews of M/V *Fug Equator*, M/V *Fugro Supporter*, and *Zhu Kezhen* for shipboard multibeam echo sounder data acquisition.

## References

Argus, D. F., R. G. Gordon, and C. DeMets (2011), Geologically current motion of 56 plates relative to the no net rotation reference frame, ***Geochem. Geophys. Geosyst.***, ***12***, Q11001, https://doi.org/10.1029/2011GC003751 (https://doi.org/10.1029/2011GC003751).

Coffin, M. F., F. A. Frey, and P. J. Wallace (2000), ***Proceedings of the Ocean Drilling Program, Initial Reports,*** vol. 183, 101 pp., Ocean Drill. Program, College Station, Texas.

Copley, J. T. (2014), Just how little do we know about the ocean floor?, ***Conversation,*** 9 Oct. 2014, http://theconversation.com/just-how-little-do-we-know-about-the-ocean-floor-327 (http://theconversation.com/just-how-little-do-we-know-about-the-ocean-floor-32751).

Karner, G. D., and N. W. Driscoll (1993), Rift flank topography and extensional basin architecture: Formation of Broken Ridge, southeast Indian Ocean, ***An. Acad. Bras. Cienc.***, ***65***, su 263–294.

Müller, R. D., M. Sdrolias, C. Gaina, and W. R. Roest (2008), Age, spreading rates, and spreading asymmetry of the world's ocean crust, ***Geochem. Geophys. Geosyst.***, ***9,*** Q04006, https://doi.org/10.1029/2007GC001743 (https://doi.org/10.1029/2007GC001743).

Mutter, J. C., and S. C. Cande (1983), The early opening between Broken Ridge and the Kerguelen Plateau, ***Earth Planet. Sci. Lett., 65,*** 369–376, https://doi.org/10.1016/0012-821X(83)90174-7 (https://doi.org/10.1016/0012-821X(83)90174-7).

Sandwell, D. T., R. D. Müller, and W. H. F. Smith (2014), New global marine gravity model from Cryo-Sat-2 and Jason-1 reveals buried tectonic structure, ***Science, 346,*** 65–67, https://doi.org/10.1126/science.1258213 (https://doi.org/10.1126/science.1258213).

Small, C., J. R. Cochran, J.-C. Sempéré, and D. Christie (1999), The structure and segmentation of the Southeast Indian Ridge, ***Mar. Geol., 161,*** 1–12, https://doi.org/10.1016/S0025-3227(99)00051-1 (https://doi.org/10.1016/S0025-3227(99)00051-1).

Weatherall, P., K. M. Marks, and M. Jakobsson (2015), A new digital bathymetric model of the world's oceans, ***Earth Space Sci.***, ***2***, 331–345, https://doi.org/10.1002/2015EA000107 (https://doi.org/10.1002/2015EA000107).

## Author Information

Kim Picard (email: kim.picard@ga.gov.au) and Brendan Brooke, Geoscience Australia, Canberra, ACT; and Millard F. Coffin, Institute for Marine and Antarctic Studies, University of Tas
Hobart, Australia; and Woods Hole Oceanographic Institution, Woods Hole, Mass.

***Editor's note: For more on how much of the seafloor under commercial flight paths remains unmapped, read this opinion piece (https://eos.org/opinions/airline-flight-path the-unmapped-ocean) on Eos.org.***

**Citation:** Picard, K., B. Brooke, and M. F. Coffin (2017), Geological insights from Malaysia Airlines flight MH370 search, *Eos, 98*, https://doi.org/10.1029/2017EO069015. Published on 06 March 2017.

# Airline Flight Paths over the Unmapped Ocean

An assessment of ocean depth knowledge underneath commercial airline routes shows just how much of the seafloor remains incognita."

Most airline passengers have no idea how little of the ocean floor beneath them has been mapped. Credit: nateemee/iStock.com

By Walter H. F. Smith, Karen M. Marks, and Thierry Schmitt 8 March 2017

It has been 3 years since Malaysia Airlines flight MH370 disappeared (http://onlinelibrary.wiley.com/doi/10.1002/2014EO210001/abstract), and no trace of it on the seafloor ha found. MH370 is believed to have deviated from its intended flight path. Yet even the typical routes taken by overseas flights are often over unknown seafloor.

Of the total over-ocean distance covered by all unique overseas flight routes, 60% is above unmapped areas.

In fact, of the total over-ocean distance covered by all unique overseas flight routes, 60% is above unmapped areas. The quality of mapping that does exist varies wi the lack of data and variance in quality hinder searches for missing aircraft, hazard assessments, and the pursuit of baseline scientific knowledge. A modest effort co lack of data.

## Uneven Coverage

Only a small percentage of Earth's seafloor has been mapped [*Copley*, 2014; *U.S. National Ocean Service*, 2014]. For example, *Smith and Marks* [2014] reported th of the southeast Indian Ocean seafloor was covered by echo soundings on 8 March 2014 when Malaysia Airlines flight MH370 went missing.

Since their publication, the MH370 search area was moved to an area where data coverage was only 1% at the time the aircraft was lost. In January 2017, the search suspended (http://minister.infrastructure.gov.au/chester/releases/2017/January/dc013_2017.aspx) after 120,000 square kilometers had been mapped (https://eos.org/project-updates/ insights-from-malaysia-airlines-flight-mh370-search) in efforts to find the aircraft. This is roughly 1/3 of the area shown in Figure 1 and 0.0336% of the area of Earth's ocean

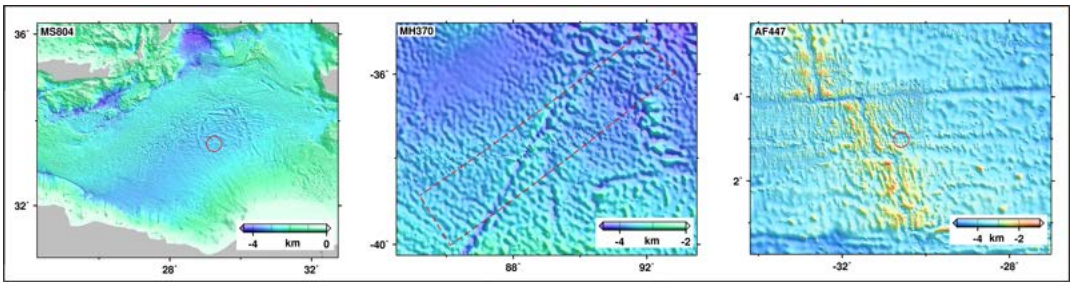


Fig. 1. From left to right, shaded relief images of the seafloor terrain in 800 × 600 kilometer regions containing the search areas for EgyptAir flight MS804, Malaysia Airlines flight MH370, and Air France flight AF447. Approximate search areas are outlined in red. Seafloor terrain models are from the *EMODnet Bathymetry Consortium* [2016] and *Weatherall et al.* [2015]. Note the variance in search area, seafloor resolution, and ship tracks over the search area.

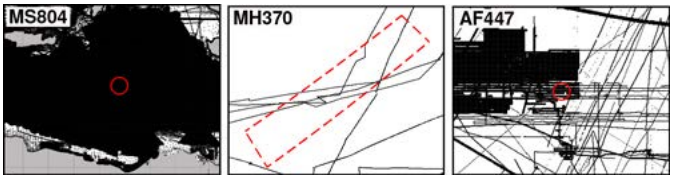


Fig. 2. Depth measurements available at the time of the EgyptAir flight MS804, Malaysia Airlines flight MH370, and Air France flight AF447 crashes (black dots).

In contrast, 86% of the eastern Mediterranean seafloor is mapped in the region where EgyptAir flight MS804 crashed on 19 May 2016, and 30% of the equatorial At mapped where Air France flight AF447 fell on 1 June 2009. Comparing these three search regions at the same scale shows that ocean mapping varies enormously fr to region (Figure 2). The AF447 search region also illustrates the strong bias toward mapping of mid-ocean ridges at the expense of other areas [*Smith*, 1998].

## Following the Airplanes

To illustrate the extent of ocean mapping under aviation routes, we compiled a list of these routes using data from the Open Flights (http://openflights.org/) project on ( These data list the originating and terminating airports of regularly scheduled commercial flights and whether or not the service is nonstop.

The actual path taken by any particular flight is determined as air traffic controllers direct each flight to a sequence of waypoints and may change as weather and tra change. We did not have this level of detail, so we approximated flight routes as great circles connecting the originating and terminating airports. Since the Open Fli do not indicate the locations of intermediate stops, we analyzed only nonstop routes.

Some pairs of airports (e.g., New York's Kennedy and London's Heathrow) are served by many airlines flying many flights in each direction, but our analysis used ea pair of airports only once, regardless of the frequency of flights between its airports.

We generated a great circle route connecting each airport pair, sampled that route every 1 kilometer of distance along its path, and then classified each sample point over mapped ocean, over unmapped ocean, or not over ocean. We found that the total distance along any individual route includes as many as 9201 kilometers flow unmapped ocean (Figure 3, left). Half of all over-ocean routes fly more than 200 kilometers over unmapped ocean, and 10% of the over-ocean routes fly more than kilometers over unmapped ocean. The longest contiguous unmapped ocean segment along any one route (Figure 3, middle) is 2293 kilometers, traveled when flying New York's John F. Kennedy and Beijing's Chongqing airports, and more than 20% of routes have a longest unmapped segment exceeding 200 kilometers. On most more than half of the over-ocean portion is over unmapped ocean (Figure 3, right).

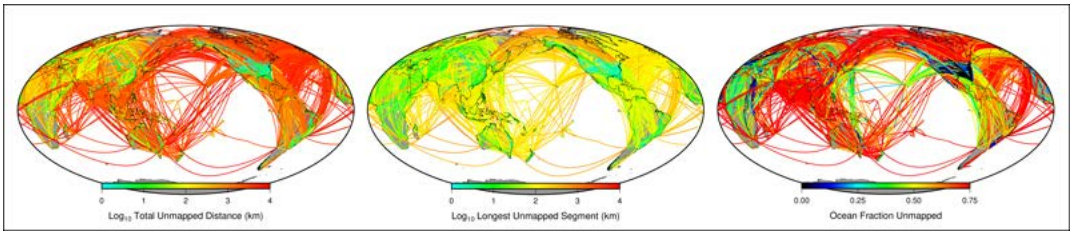


Fig. 3. Great circle routes of commercial airline flights, showing (left) total distance along each route that is over unmapped ocean, (middle) the longest segment of any route that is over unmapped ocean, and (right) the relative

fraction of each route that is over unmapped ocean (ratio of total unmapped ocean distance to total ocean distance).

We found a total of 19,024 unique nonstop routes. Of these, 11,665 fly at least 1 kilometer over ocean, and 10,686 fly at least 1 kilometer over unmapped ocean. The distance is slightly more than 33.4 million kilometers, 33% of which is over ocean, with 60% of the total over-ocean distance being over unmapped ocean. These nu not indicate the probability that an aircraft or a passenger is over unmapped ocean because our analysis is unable to account for the number of aircraft and passeng each route over a given period of time.

## Our Criteria

An analysis like our airline route survey has to define how many depth readings it takes to list an area as mapped. Depth measurements that can be readily obtained without specialized access, licensing, or payment, which we call "available" data, are quite variable in their sampling density and in the age, technology, and accurac sounding and navigation systems used. All these variations are irregularly distributed over the globe [*Smith*, 1993; *Wessel and Chandler*, 2011].

We divided the global seafloor area into equal-area square tiles 1 nautical mile on a side and considered any tile mapped if it contained one or more available echo s For context, modern hull-mounted multibeam echo sounders (MBES) map a swath of the ocean along the ship's path, but the vast majority of available data (95% o by area) are point values—one depth measurement at one place, typically an analog measurement made by a wireline or a single-wide-beam acoustic sounder [*Smit*

Only 8% of the global ocean is mapped.

Our method produces a generous overestimate, with some tiles having only one sounding. Also, the majority of available data are poorly navigated and error prone [ 1993; *Wessel and Chandler*, 2011]. Even by this generous definition, however, only 8% of the global ocean is mapped [*Wessel and Chandler*, 2011, Figure 8].

In the 92% of ocean area where depth has not been measured, satellite altimetry interpolates the gaps between available soundings [*Smith and Sandwell*, 1997; *Bec* 2009; *Weatherall et al.*, 2015]. This approximation strongly underestimates seafloor topography and roughness [*Becker and Sandwell*, 2008], with a variety of con that affect sciences, from earthquake and tsunami hazard assessment [*Mofjeld et al.*, 2004] to ocean circulation [*Gille et al.*, 2004] and mixing [*Kunze and Llewelly* 2004] and climate forecasts [*Jayne et al.*, 2004].

## Addressing the Data Shortage

All of Earth's ocean floors deeper than 500 meters could be mapped at a total cost of $2–3 billion.

All of Earth's ocean floors deeper than 500 meters (i.e., exclusive of territorial waters and continental shelves) could be mapped by GPS-navigated MBES for 200 sh effort (e.g., 40 ships working for 5 years), at a total cost of US$2–3 billion [*Carron et al.*, 2001]. According to the NASA scientists we consulted, this is less than the NASA's next mission to Europa.

We hope that our survey of the state of ocean mapping from the perspective of over-ocean flight routes makes the relevance of ocean mapping and the current lack o information clear to the public.

## Acknowledgments

Comments by two anonymous reviewers improved the manuscript. The views expressed here are solely those of the authors and do not constitute a statement of pol decision, or position on behalf of NOAA or Service Hydrographique et Oceanographique de la Marine or the U.S. or French governments.

## References

Becker, J. J., and D. T. Sandwell (2008), Global estimates of seafloor slope from single-beam ship soundings, ***J. Geophys. Res., 113***, C05028, https://doi.org/10.1029/2006JC003879 (https://doi.org/10.1029/2006JC003879).

Becker, J. J., et al. (2009), Global bathymetry and elevation data at 30 arc seconds resolution: SRTM30PLUS, ***Mar. Geod., 32***(4), 355–371, https://doi.org/10.1080/0149041090329776 (https://doi.org/10.1080/01490410903297766).

Carron, M. J., P. R. Vogt, and W.-Y. Jung (2001), A proposed international long-term project to systematically map the world's ocean floors from beach to trench: GOMaP (Global Ocean Mapping Program), ***Int. Hydrogr. Rev., 2***(3), 49–55.

Copley, J. (2014), Just how little do we know about the ocean floor?, ***Sci. Am.***, 9 October 2014, http://www.scientificamerican.com/article/just-how-little-do-we-know-about-the-ocean (http://www.scientificamerican.com/article/just-how-little-do-we-know-about-the-ocean-floor/).

EMODnet Bathymetry Consortium (2016), EMODnet digital bathymetry (DTM), http://doi.org/10.12770/c7b53704-999d-4721-b1a3-04ec60c87238 (http://doi.org/10.12770/c7b53704-999d-4721-b1a3-04ec60c87238).

Gille, S. T., E. J. Metzger, and R. Tokmakian (2004), Seafloor topography and ocean circulation, ***Oceanography***, ***17***(1), 47–54, https://doi.org/10.5670/oceanog.2004.66 (https://doi.org/10.5670/oceanog.2004.66).

Jayne, S. R., L. C. St. Laurent, and S. T. Gille (2004), Connections between ocean bottom topography and Earth's climate, ***Oceanography***, ***17***(1), 65–74, https://doi.org/10.5670/oceanog.2004.68 (https://doi.org/10.5670/oceanog.2004.68).

Kunze, E., and S. G. Llewellyn Smith (2004), The role of small-scale topography in turbulent mixing of the global ocean, ***Oceanography***, ***17***(1), 55–64, https://doi.org/10.5670/oceanog.2004.67 (https://doi.org/10.5670/oceanog.2004.67).

Mofjeld, H. O., et al. (2004), Tsunami scattering and earthquake faults in the deep Pacific Ocean, ***Oceanography***, ***17***(1), 38–46, https://doi.org/10.5670/oceanog.2004.65 (https://doi.org/10.5670/oceanog.2004.65).

Smith, W. H. F. (1993), On the accuracy of digital bathymetric data, ***J. Geophys. Res., 98***(B6), 9591–9603, https://doi.org/10.1029/93JB00716 (https://doi.org/10.1029/93JB00716).

Smith, W. H. F. (1998), Seafloor tectonic fabric from satellite altimetry, ***Annu. Rev. Earth Planet. Sci.***, ***26***, 697–747, https://doi.org/10.1146/annurev.earth.26.1.697 (https://doi.org/10.1146/annurev.earth.26.1.697).

Smith, W. H. F., and K. M. Marks (2014), Seafloor in the Malaysia Airlines flight MH370 search area, ***Eos Trans. AGU***, ***95***(21), 173–174, https://doi.org/10.1002/2014EO210001 (https://doi.org/10.1002/2014EO210001).

Smith, W. H. F., and D. T. Sandwell (1997), Global seafloor topography from satellite altimetry and ship depth soundings, ***Science 277***(5334), 1956–1962, https://doi.org/10.1126/science.277.5334.1956 (https://doi.org/10.1126/science.277.5334.1956).

U.S. National Ocean Service (2014), How much of the ocean have we explored?, http://oceanservice.noaa.gov/facts/exploration.html (http://oceanservice.noaa.gov/facts/exploration.html).

Weatherall, P., et al. (2015), A new digital bathymetric model of the world's oceans, ***Earth Space Sci.***, ***2***(8), 331–345, https://doi.org/10.1002/2015EA000107 (https://doi.org/10.1002/2015EA

Wessel, P., and M. T. Chandler (2011), The spatial and temporal distribution of marine geophysical surveys, ***Acta Geophys.***, ***59***(1), 55–71, https://doi.org/10.2478/s11600-010-0038-1 (https://doi.org/10.2478/s11600-010-0038-1).

—Walter H. F. Smith (email: walter.hf.smith@noaa.gov (mailto:Walter.HF.Smith@noaa.gov)) and Karen M. Marks, Laboratory for Satellite Altimetry, National Oceanic and Atmospheric Administration, College Park, Md.; and Thierry Schmitt, Service Hydrographique et Oceanographique de la Marine, Brest, France

***Editor's note: For more on efforts to map the seafloor in the search area for Malaysia Airlines flight MH370, read this project update (https://eos.org/project-updates/ge insights-from-malaysia-airlines-flight-mh370-search) on Eos.org.***

**Citation:** Smith, W. H. F., K. M. Marks, and T. Schmitt (2017), Airline flight paths over the unmapped ocean, *Eos, 98,* https://doi.org/10.1029/2017EO069127. Published on 08 March 2017.



---